Environmental Design Revitalization Model of Ancient Villages Based on Cultural Landscape Regeneration

Yanfei Zhou[1,*], Yikang Yan[1]
[1]School of Design and Art, Shandong Huayu University of Technology, Dezhou 253034, China
Corresponding author: Yanfei Zhou (e-mail: jianjian1109168@163.com).

ABSTRACT Ancient village cultural landscapes face a structural disconnect between traditional construction wisdom and contemporary living needs, urgently requiring a shift from passive landscape preservation to proactive environmental design revitalization. This paper adopts a technical framework that couples spatial syntax, landscape ecology, and multi-agent simulation, proposes a three-stage activation path, constructs a digital twin model, and diagnoses spatial topological defects by calculating the integration degree and selectivity of the axis diagram. It employs a gravity model to assess the connectivity and vulnerability of cultural patches, and utilizes ENVI-met microclimate simulation and social force model behavioral flow simulation to achieve multi-objective Pareto optimization of thermal environment and spatial vitality. In empirical cases, spatial network optimization increased the average global integration degree of core nodes from 0.922 to 1.213 and the local integration degree from 0.986 to 1.3685. The fusion degree of 978 components extracted from the skeleton and encoded using shape context clustering increased by an average of 34.18% under the activation mode, and the utilization efficiency of intangible cultural heritage space display increased by an average of 42.34%. The research shows that the activation mode coupling digital gene encoding and behavioral simulation can effectively repair spatial fractures in ancient villages and activate the cultural regeneration potential of daily living spaces, providing a generalizable methodological path for the protection of similar heritage.

INDEX TERMS Cultural landscape regeneration; Ancient village environmental design; Spatial syntax; Cultural gene implantation

I. INTRODUCTION

UNDER the dual drive of current rural revitalization and the inheritance and development of excellent traditional Chinese culture, ancient villages, as a typical paradigm of cultural landscapes in the agricultural civilization period, have evolved from a single issue of cultural relic restoration to a comprehensive social proposition related to regional identity recognition and community sustainable development in terms of protection and regeneration. However, the real dilemma lies in the fact that a large number of ancient villages are experiencing a polar swing between "frozen" preservation of their appearance and disorderly tourism development. The spatial topology logic, microclimate adaptability strategy, and symbolic semantic system contained in traditional construction wisdom are difficult to effectively meet the practical needs of improving the quality of life and functional iteration in contemporary rural areas. The coexistence of "spatial fragmentation" and "genetic discontinuity" in this deep fracture makes it urgent for the revitalization of ancient village environmental design to break through empirical and fragmented intervention models, and shift towards a new methodological framework that combines scientific diagnostic accuracy and system coupling depth.

This article constructs a high-precision digital twin model of ancient villages, introducing spatial syntactic topology reconstruction and landscape ecology network analysis into the field of cultural heritage. It achieves accurate quantitative interpretation of street and alley integration, cultural patch connectivity, and edge degradation nodes, solving the problem of traditional field surveys being difficult to capture deep-seated spatial structural lesions. Secondly, using skeleton extraction and shape context clustering algorithms, traditional building components and pavement patterns are encoded into reusable and adaptable spatial syntax units, thus building a semantic bridge between traditional construction logic and modern functional spaces. Finally, the ENVI-met microclimate simulation and the behavioral flow simulation of the social force model are placed in the same framework, and the NSGA-II multi-objective genetic algorithm is used to drive the Pareto synergistic optimization of thermal environmental benefits and cultural vitality index, so that the activation scheme can move from static blueprint to dynamic adaptation.

The structure of the article is as follows: This article systematically reviews the world research progress in the field of cultural landscape regeneration and environmental design activation, defines the theoretical basis and methodological boundaries of this study; This article elaborates on research methods, including case selection criteria and multi-source data collection fusion, quantitative diagnostic methods for cultural landscape spatial structure, and mathematical modeling and algorithm implementation of the three-stage activation technology route of "spatial network optimization cultural gene implantation multi-objective coupling simulation"; This article takes typical ancient villages as empirical objects, presents the experimental results and discusses the benefits of optimizing spatial topology structure and deeply integrating material and intangible cultural heritage; This article summarizes the research conclusions, extracts the methodological universality value of this activation mode, and points out the expansion direction of future research.

II. RELATED WODR

As the core carrier of cultural landscapes, ancient villages are facing a profound rupture between traditional construction wisdom and contemporary living needs. How to shift from passive style preservation to active environmental design activation has become an urgent methodological proposition in the intersection of cultural heritage and landscape regeneration. Mohajer Milani and Assarzadeh [1] validated the applicability of a responsive environmental design framework in historical commercial composite spaces by constructing a multi-level evaluation index system and applying it to Tajrish Square in Tehran. Ibrahim et al. [2] introduced spatial modeling and interpolation techniques into the preliminary analysis of landscape design to enhance the scientific response capability of design decisions to the spatial heterogeneity of environmental factors. Liu and Zhang [3] extracted a regional environmental design method model of "local wisdom+modern translation+community empowerment" through field investigations and design experiments on multiple typical ancient villages in Zhejiang. Chen [4] proposed the establishment of a digital knowledge base and an adaptive translation path to effectively integrate traditional construction logic with the contemporary national spatial planning system, providing a complete methodological chain from prototype analysis to institutional promotion for the planning and inheritance of ancient villages in Huizhou and even across the country. Taking Lijia Village in Xihu, Nanchang City as a precise starting point, Yang and Dong [5] used the Kano model to scientifically rank the landscape renovation needs of multiple stakeholders, and successfully designed and implemented a micro renewal landscape renovation plan that takes into account the protection of Huizhou style, restoration of ecological water systems, and integration of modern living functions.

Brown and Gabrys [6] constructed a systematic participation framework covering five dimensions: shared vision construction, knowledge coexistence, flexible governance, capacity building, and continuous feedback, through a systematic review and in-depth comparison of community led landscape regeneration projects worldwide. Barbanente and Grassini [7] revealed that the key to the success of landscape regeneration in marginal areas lies in elevating it from physical spatial beautification to a systematic engineering of "social economic governance". Tzortzi et al. [8] combined landscape feature assessment with scenario planning methods to transform agricultural cultural heritage from a development constraint factor into a strategic core resource for landscape regeneration in peripheral areas. Cobeñas as et al. [9] demonstrated that ecological restoration and community livelihood improvement can achieve a highly synergistic win-win situation through low impact tourism design and assisted natural succession strategies. Septian [10] revealed that the identity of small-scale village landscapes is actually rooted in daily practice landscape networks such as field paths, public wells, and temporary barns, and proposed incorporating intergenerational dialogue mechanisms into the process of regeneration design. The environmental physical effects and behavioral flow responses of the activation schemes mentioned above often belong to different disciplinary discourse systems, which makes it difficult for existing models to predict intervention effects and adaptively adjust strategies in response to complex cultural landscape regeneration propositions. Based on this, this study attempts to construct a closed-loop activation path that integrates digital twin modeling, spatial syntactic diagnosis, cultural gene clustering, and multi-agent coupling simulation, in order to provide a methodological tool for the design of ancient village environments that combines quantitative accuracy and system adaptability.

III. METHOD

A. OVERVIEW OF THE RESEARCH AREA AND DATA COLLECTION

The selection of case villages is based on three quantitative criteria: spatial pattern integrity, historical building survival rate, and degree of commercial intervention [11]. The integrity of spatial pattern requires a retention rate of no less than 70% for the texture of streets and alleys during the Ming and Qing dynasties, calculated through the overlay comparison of historical topographic maps and current aerial images. Assuming the total length of streets and alleys in the Ming and Qing dynasties in the historical topographic map is L_h, and the corresponding identifiable length of streets and alleys in the current aerial images is L_s, the formula for calculating the retention rate of street texture η_{street} is:

$$\eta_{\text{street}} = \frac{L_s}{L_h} \times 100\%. \tag{1}$$

η_{street} is the retention rate of street and alley texture, L_s is the total length of Ming and Qing streets and alleys preserved in the current situation, and L_h is the total length of Ming and Qing streets and alleys recorded in history.

The survival rate of historical buildings is based on the registration list of the third national cultural relics census, and it is confirmed that the proportion of traditional style buildings in the core protected area exceeds 65%. The total number of traditional style buildings registered in the protected area is $N_{\text{registered}}$, of which the number of buildings with well preserved styles is $N_{\text{preserved}}$. The formula for calculating the survival rate η_{heritage} is:

$$\eta_{\text{heritage}} = \frac{N_{\text{preserved}}}{N_{\text{registered}}} \times 100\%. \tag{2}$$

η_{heritage} is the survival rate of historical buildings, $N_{\text{preserved}}$ is the number of well preserved traditional buildings, and $N_{\text{registered}}$ is the total number of registered traditional style buildings.

The degree of commercial intervention is determined by a comprehensive evaluation of the density of shops along the street and the volume index of newly built buildings. Villages that have experienced the construction of tourism supporting facilities in the past five years and have shown typical street and alley interface fractures are selected. The density of shops along the street, ρ_{shop}, is defined as $\rho_{\text{shop}} = N_{\text{shop}}/L_{\text{street}}$, where N_{shop} is the total number of commercial shops along the street within the core protected area, and L_{street} is the total length of streets and alleys (km). The new building volume index V_{new} is calculated using the volume ratio method: $V_{\text{new}} = \sum V_{\text{new\_bldg}} / \sum V_{\text{total\_bldg}}$. A ratio exceeding 0.15 is considered significant intervention, where $V_{\text{new\_bldg}}$ represents the volume of each new building and $V_{\text{total\_bldg}}$ represents the total volume of each building within the protected area. In addition, the case village should include no less than two active intangible cultural heritage projects, and there should be significant spatial overlap between the daily life trajectories of residents and the tourist flow lines, in order to meet the modeling needs of multi-agent simulation for the diversity of behavioral subjects [12].

The data was collected using the DJI M300 RTK drone equipped with Zenmuse L1 LiDAR, with a relative altitude of 80 meters. The heading overlap rate and lateral overlap rate were 70% and 60%, respectively. The pulse transmission frequency was set to 240 kHz, and the theoretical point cloud density reached 50 points per square meter. Assuming the total coverage area of the drone flight is A_{survey} (m^2), the pulse transmission frequency is f_{pulse} (Hz), the flight speed is v_{UAV} (m/s), and the flight band width is w_{strip} (m), the estimated theoretical density of the point cloud ρ_{point} is:

$$\rho_{\text{point}} = \frac{f_{\text{pulse}}}{v_{\text{UAV}} \cdot w_{\text{strip}}} \times \eta_{\text{overlap}}. \tag{3}$$

ρ_{point} is the theoretical density of the point cloud (points/m^2), f_{pulse} is the frequency of laser radar pulse emission, v_{UAV} is the flight speed of the drone, w_{strip} is the width of the flight band, and η_{overlap} is the comprehensive factor of heading and lateral overlap rate, with a value of 0.42.

The ground control points are measured using a Leica GS18 GNSS receiver, with a mean square error between the plane and elevation controlled within 5 centimeters. They are used as initial transformation parameters for the iterative nearest neighbor point algorithm in point cloud registration. Multispectral acquisition uses the RedEdge MX dual camera system, covering five bands: blue (475 nm), green (560 nm), red (668 nm), red edge (717 nm), and near-infrared (842 nm). The ground resolution is set to 10 centimeters, and the acquisition time is selected between 10:00 and 14:00 local time to ensure illumination consistency. The point cloud preprocessing performs noise filtering and ground point classification, using progressive encryption triangulation filtering algorithm to extract ground points, and the building facade point cloud is segmented through random sampling consistency algorithm. After radiometric calibration and DOS1 atmospheric correction of spectral images, a random forest classifier (with 100 decision trees and a minimum of 5 leaf nodes) is used to generate a grid of land cover categories. The material attributes are mapped to the vertices of the 3D mesh using the nearest neighbor assignment method, forming a digital twin model with dual annotations of geometry and material [13], [14].

B. QUANTITATIVE DIAGNOSTIC METHODS FOR CULTURAL LANDSCAPE SPATIAL STRUCTURE

Based on the digital twin model extraction of street and alley centerlines, an axis map is constructed in DepthmapX software to convert all publicly accessible linear spaces within the ancient village into an axis model. The integration degree is calculated using radius angles Radius=n (global) and Radius=3 (local, corresponding to a 3-minute walking range), and the output values are standardized to eliminate the influence of differences in the number of axes. If the total number of axes in the axis map is n, and the shortest path distance from any axis i to all other axes is d_{ij}, then the global integration degree I_i is:

$$I_i = \frac{n \cdot \left(\log_2\left(\frac{n+2}{3}\right) + 1\right)}{(n-1) \cdot \sum_{j=1}^{n} d_{ij}}. \tag{4}$$

The local integration degree is limited by the topological distance with a radius of Radius=3, which only counts the set of axes $R_3(i)$ within three steps from axis i:

$$I_i(3) = \frac{|R_3(i)| \cdot \left(\log_2\left(\frac{|R_3(i)|+2}{3}\right) + 1\right)}{(|R_3(i)| - 1) \cdot \sum_{j \in R_3(i)} d_{ij}}. \tag{5}$$

$I_i(3)$ is the local integration degree of axis i.

The selection degree reflects the probability of any axis being traversed as the shortest path, and the search radius is set to 400 meters during calculation, corresponding to the typical spatial scale of daily activities in the village. If the number of times the axis i is traversed as the shortest path

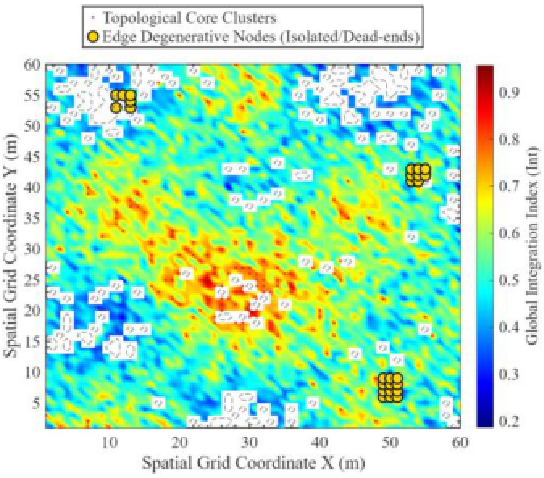

FIGURE 1. Spatial Syntax Topology Reconstruction and Edge Degradation Node Diagnosis of Ancient Villages

within the search radius r is $N_{\text{choice}}(i, r)$, then the selection degree $C_i(r)$ is:

$$C_i(r) = \frac{\log(1 + N_{\text{choice}}(i, r))}{\log(1 + \bar{N}_{\text{choice}}(r))}. \tag{6}$$

$\bar{N}_{\text{choice}}(r)$ is the geometric average of the number of times all axes within radius r have been traversed.

View analysis runs on a two-dimensional grid with a grid sampling interval of 2 meters, and outputs two parameters: view area and view integration. The identification rule for the core of spatial structure is defined as a set of axes with a global integration degree higher than the global mean plus one standard deviation, and this set forms a continuous closed or semi closed topological cluster in space. The edge degradation node is determined as an isolated axis with a selection degree lower than the mean minus one standard deviation, and a connectivity degree less than 2. Such axes usually correspond to abandoned tunnels or forced blocked dead end roads. Based on the above mathematical rules, topological reconstruction of the centerline grid of streets and alleys is implemented, and the structural grading state of the entire space presents a visually heterogeneous distribution. By quantitatively calculating the morphological variables of the axis model, the distribution characteristics of the dead corner space and the core access path are clearly defined in the spatial coordinate system, forming the diagnostic results shown in Fig. 1.

Figure 1 presents the global integration chromatographic distribution and spatial localization of structural degradation points in the internal street network of the ancient village. The color of the base map, from red to blue, represents the decreasing trend of global integration values from high to low. The continuous axis lines concentrated in the red area form the topological core cluster that dominates the overall vitality of the village. The isolated dots marked in gold represent edge degradation nodes with a selectivity lower than the mean minus one standard deviation and a connectivity less than 2, which precisely indicate the location where spatial fragmentation blocking occurs.

The landscape ecology network model divides the cultural space of ancient villages into four types of patches: ancestral worship, commercial markets, residential life, and folk exhibitions. The patch boundaries are directly extracted from the digital twin's land classification grid, and the minimum patch area threshold is set to 50 square meters. When calculating the interaction force between patches using the gravity model, the patch quality parameter is taken as the product of the patch area and the mean global integration degree of spatial syntax. The distance between patches is determined by the centroid Euclidean distance, and the friction coefficient is weighted based on the ground paving material of the connecting path. Assuming the areas of patches a and b are S_a and S_b, respectively, the global integration mean is $\bar{I}_a$ and $\bar{I}_b$, the Euclidean distance between the centroids is D_{ab}, and the friction coefficient is μ_{ab}, then the gravitational force F_{ab} between patches is:

$$F_{ab} = \frac{(S_a \cdot \bar{I}_a) \cdot (S_b \cdot \bar{I}_b)}{\mu_{ab} \cdot D_{ab}^2}. \tag{7}$$

The connectivity assessment was completed in Conefor Sensinode 2.6 software, calculating the overall connectivity index and probability connectivity index. Assuming the total number of cultural patches is m, the maximum connection probability between patches a and b is p_{ab}, and the connection distance threshold is set to 200 meters, the overall connectivity index IIC is:

$$\text{IIC} = \frac{\sum_{a=1}^{m} \sum_{b=1}^{m} \frac{(S_a \cdot \bar{I}_a) \cdot (S_b \cdot \bar{I}_b)}{1 + c_{ab}}}{\left(\sum_{a=1}^{m} S_a \cdot \bar{I}_a\right)^2}. \tag{8}$$

c_{ab} is the number of intermediate nodes on the shortest path connecting patches a and b.

The probability connectivity index PC is:

$$\text{PC} = \frac{\sum_{a=1}^{m} \sum_{b=1}^{m} (S_a \cdot \bar{I}_a) \cdot (S_b \cdot \bar{I}_b) \cdot p_{ab}}{\left(\sum_{a=1}^{m} S_a \cdot \bar{I}_a\right)^2}. \tag{9}$$

The vulnerability assessment adopts the node deletion method, which removes each cultural patch in sequence and recalculates the percentage decrease of IIC. If the overall connectivity index after removing patch q is IIC_{-q}, then the vulnerability of patch q, denoted as ν_q, is:

$$\nu_q = \frac{\text{IIC} - \text{IIC}_{-q}}{\text{IIC}} \times 100\%. \tag{10}$$

Define the top 30% descending patches as high vulnerability nodes to guide the selection of priority intervention objects in subsequent spatial network optimization.

C. DESIGN METHOD FOR THREE STAGE ACTIVATION TECHNOLOGY ROUTE

The optimization of spatial networks is based on the global integration index as the core basis for the reclassification of street and alley levels. Set the top 15% of the integrated axis as the main travel line, the middle 60% as the secondary connecting line, and the last 25% as the landscape trail. If the global integration degree of axis i is I_i, and the set of integration degrees for all axes is $I = \{I_1, I_2, \dots, I_n\}$, then the set of backbone lines M_{primary} is:

$$M_{\text{primary}} = \{i \mid I_i \geq Q_{0.85}(I)\}. \tag{11}$$

$Q_{0.85}(I)$ is the 85th percentile of the set.

The secondary connection line set $M_{\text{secondary}}$ and the landscape trail set M_{trail} are respectively:

$$\begin{aligned} M_{\text{secondary}} &= \{i \mid Q_{0.25}(I) \leq I_i < Q_{0.85}(I)\}, \\ M_{\text{trail}} &= \{i \mid I_i < Q_{0.25}(I)\}. \end{aligned} \tag{12}$$

$Q_{0.25}(I)$ is the 25th percentile. For the detected edge degradation nodes, in locations where their connectivity is less than 2 and their selectivity is low, the spatial coupling is improved by adding intersection points between secondary connecting lines and main lines. The principle for selecting intersection points is that the length of the newly added connecting line should not exceed 15 meters and does not involve the demolition of historical buildings. The accessibility improvement of core cultural nodes (ancestral halls, stages, important gatehouses) is achieved by adjusting the hierarchy of adjacent axes: if the local integration degree of a core node at Radius=3 is lower than the global median, its adjacent landscape trails can be upgraded to secondary connecting lines, ensuring that each core node is connected to at least two different levels of axes within a 3-minute walk. If the local integration degree of the core node c is $I_c(3)$ and the global median is $\tilde{I}(3)$, then the upgrade condition is $I_c(3) < \tilde{I}(3)$, where c is the index of the core cultural node and $\tilde{I}(3)$ is the median of the local integration degrees of all axes. The optimized axis network is re inputted into DepthmapX to verify the integration and selection distribution. If the standard deviation is not reduced below the preset threshold, the connection strategy is adjusted to form a closed topology optimization loop.

The extraction of material cultural genes is based on the three-dimensional grid of building components and pavement patterns in digital twins. The skeleton extraction algorithm is used to obtain the geometric topology structure, and then the shape context descriptors are clustered and encoded to form a reusable cultural gene library. Let the extracted set of 3D mesh vertices for a certain building component be $P = \{p_1, p_2, \dots, p_N\}$, and the topology structure obtained after skeleton extraction be the graph $G_{\text{gene}} = (V_{\text{gene}}, E_{\text{gene}})$, where G_{gene} is the skeleton topology graph, V_{gene} is the set of skeleton nodes, and E_{gene} is the set of skeleton edges. The calculation method of the shape context descriptor for the skeleton node $v \in V_{\text{gene}}$ is as follows: the histogram h_v of the distribution of each sector and other nodes within the radius interval of the node in the polar coordinate system is calculated, and the formula for calculating the shape similarity χ^2_{uv} between the two skeleton nodes u and v is:

$$\chi^2_{uv} = \frac{1}{2} \sum_{k=1}^{K} \frac{(h_u(k) - h_v(k))^2}{h_u(k) + h_v(k) + \epsilon}. \tag{13}$$

h_u and h_v are the shape context histograms of the corresponding nodes, k is the sector index, K is the total number of sectors, ϵ is a very small positive number, and χ^2_{uv} is the shape similarity. By spectral clustering, components with a shape context distance of less than the threshold value of χ^2_{uv} are classified as belonging to the same cultural gene type. The matching of intangible cultural heritage activities (such as traditional opera and handicrafts) with spatial requirements adopts the functional matrix method. The row vectors of the matrix represent the types of intangible cultural heritage projects, and the column vectors represent three hard indicators: spatial opening scale, top interface height, and interface enclosure degree.

The simulated boundary layer height of ENVI-met V5 is set to 50 meters, with a horizontal grid resolution of 2 meters by 2 meters. The vertical layers are densified to 1 meter intervals near the ground (0-5 meters), and the above layers are increased by a factor of 1.5. Simulate typical summer weather days (6:00 to 19:00), with initial temperature, relative humidity, and wind speed set based on historical extreme values in the case area. The underlying surface material properties are directly assigned values from the spectral classification results of the digital twin. The behavior flow model uses a social force model to simulate individual movement, and the parameters of self driving force, repulsive force, and attraction are taken as Helbing's classic calibration values. Assuming the mass of individual α is m_α, the expected velocity is v^0_α, the current velocity is v_α, the expected direction of motion is e^0_α, and the relaxation time is τ_α, then the self driving force F^{self}_α is:

$$F^{\text{self}}_\alpha = m_\alpha \cdot \frac{v^0_\alpha e^0_\alpha - v_\alpha}{\tau_\alpha}. \tag{14}$$

The inter individual repulsive force $F^{\text{rep}}_{\alpha\beta}$ is:

$$F^{\text{rep}}_{\alpha\beta} = A_\alpha \cdot \exp\left(\frac{r_{\alpha\beta} - d_{\alpha\beta}}{B_\alpha}\right) \cdot n_{\alpha\beta}. \tag{15}$$

β is the index of another individual, A_α and B_α are the parameters of repulsive force intensity and range of action, $r_{\alpha\beta}$ is the sum of the radii of the two bodies, $d_{\alpha\beta}$ is the distance between the centroids, and $n_{\alpha\beta}$ is the unit vector pointing from β to α.

The coupling implementation method is spatial grid mapping: the grid by grid predicted average voting (PMV) value output by ENVI met is normalized and used as an additional term for the path selection cost function in the social force model. If the original PMV value of grid g is PMV_g and normalized to $\widehat{\text{PMV}}_g \in [0, 1]$, then the path selection cost Cost_g of grid g is:

$$\text{Cost}_g = (1 - \lambda) \cdot \text{Cost}^{\text{base}}_g + \lambda \cdot \widehat{\text{PMV}}_g. \tag{16}$$

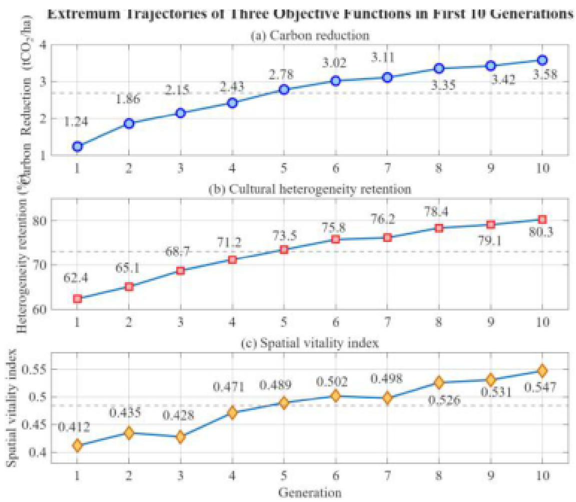

FIGURE 2. Extreme Trajectory of Population Objective Function

$\text{Cost}_g^{\text{base}}$ is the basic path cost (positively correlated with path length), and λ is the weight coefficient of thermal environment cost (taken as 0.4). Multi-objective optimization aims to maximize carbon emission reduction benefits (equivalent to vegetation transpiration and building energy consumption), cultural heterogeneity retention rate (cultural gene spatial distribution diversity index), and spatial vitality index. The NSGA-II algorithm is called on the Matlab platform, with a population size of 50, maximum evolutionary generations of 100, crossover probability of 0.8, and mutation probability of 0.1. If the t-th generation Pareto front is P_t and the hypervolume value is $\mathcal{H}_t$, then the termination condition for the iteration is:

$$\frac{|\mathcal{H}_t - \mathcal{H}_{t-20}|}{\mathcal{H}_{t-20} + \epsilon} < 0.005. \tag{17}$$

Terminate the iteration when the average hypervolume change rate of the Pareto front for 20 consecutive generations is less than 0.5%. Figure 2 records the population extremum trajectories of each objective function in the first 10 generations to verify the convergence direction of early search and the robustness of parameter configuration startup.

IV. RESULTS AND DISCUSSION

A. OVERVIEW OF THE EMPIRICAL OBJECT

This study selects a typical ancient village as the empirical object. The village was first built in the Southern Tang Dynasty of the Five Dynasties. The "seven vertical and one horizontal" street and alley texture of the Ming and Qing dynasties has a retention rate of over 85%. There are 297 existing traditional buildings and ruins of the Ming and Qing dynasties, and the proportion of traditional style buildings in the core protected area exceeds 85%. In recent years, the construction of tourism supporting facilities has resulted in a new building volume index of approximately 0.18-0.22, with significant commercial involvement. The space is arranged in a comb like pattern, with cobblestone alleys and underground drainage systems, and exquisitely decorated brick

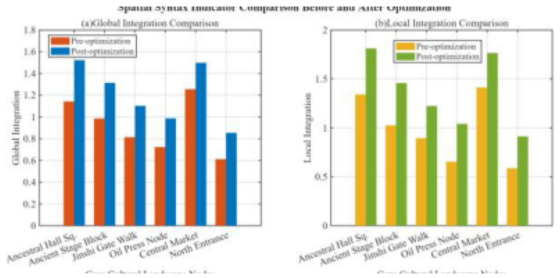

FIGURE 3. Spatial Syntactic Indicators of Core Cultural Landscape Nodes Before and After Optimization

and wood structures. At present, 189 national protected buildings have been repaired, but problems such as visual interference from municipal cables, insufficient maintenance of non-national protected buildings, broken interfaces in new construction, and weak inheritance of a provincial-level intangible cultural heritage site coexist, making it a typical case for diagnosing "spatial fragmentation" and "marginal degradation nodes".

B. OPTIMIZATION OF SPATIAL TOPOLOGY STRUCTURE

By performing a two-level relaxation iteration calculation on the topology layers of the street and alley centerlines before and after optimization, the global integration degree and local integration degree change data of the core cultural landscape nodes were obtained, as shown in Fig. 3.

After optimization, the global integration and local integration of all nodes showed a significant increase. The average global integration of the six nodes increased from 0.922 to 1.213 (an increase of 31.6%), and the average local integration increased from 0.986 to 1.3685 (an increase of 38.8%). The embedding of secondary connecting lines effectively reduces the depth of topology, incorporates edge nodes into the main radiation range, significantly improves the accessibility balance of the ancient village street network, and provides structural support for the uniform flow of subsequent behavior.

C. DEEP INTEGRATION BENEFITS OF MATERIAL AND NON-MATERIAL CULTURES

The skeleton extraction algorithm (sampling interval of 0.05 m, minimum branch length of 0.30 m) is used to extract the centerline topology of the component, and the shape context descriptor is set with 12 polar coordinate sectors and 5 radius intervals. The fusion degree is defined as the number of matching components divided by the theoretical maximum capacity. The traditional mode is the original layout, while the activation mode is the optimized implantation guided by the gene library. After classifying and statistical analysis of 978 components, the evaluation results of cultural gene spatial integration were obtained as shown in Table 1.

TABLE 1. Cultural Gene Spatial Integration Degree Assessment

Component Type	Sample Size (n)	Traditional Mode Integration	Activated Mode Integration	Improvement Rate (%)
Beam frame	187	0.53	0.72	35.8
Spandrel bracket	234	0.48	0.64	33.3
Column base	156	0.61	0.82	34.4
Gate tower	89	0.44	0.59	34.1
Pavement	312	0.57	0.76	33.3

The fusion degree of the five types of components in the activated mode is significantly higher than that in the traditional mode, with an average improvement rate of 34.18%. The beam frame has the largest lifting amplitude (35.8%), due to its high recognition and strong matching as a load-bearing skeleton in space; The absolute value of column foundation fusion is the highest (0.82 after activation), reflecting its geometric properties of easy position adaptation and style reuse as an independent base component. Although the paving has the largest sample size (312), the improvement rate is relatively low (33.3%) due to the constraints of ground continuity and drainage slope. Overall, shape context clustering can effectively encode discrete components into reusable gene units, enabling gene pool guided implantation strategies to achieve stable positive gains across all types of components.

Using five types of spaces including ancestral worship, commercial markets, residential life, folk exhibitions, and mixed transitions as sampling units, three representative measurement points were selected for each type. The behavior annotation method (observation period 8:00-17:00, recorded every 30 minutes) was used to count the number of residents and spatial usage duration of intangible cultural heritage related activities. Before and after the implementation of the activation strategy, 15 effective observation days can be collected each (excluding rainy days and festival days), and the utilization rate is calculated as the daily average number of visitors multiplied by the average duration of stay divided by the rated capacity of the space. Figure 4 shows a comparison of the utilization efficiency of intangible cultural heritage space display between traditional and activated modes.

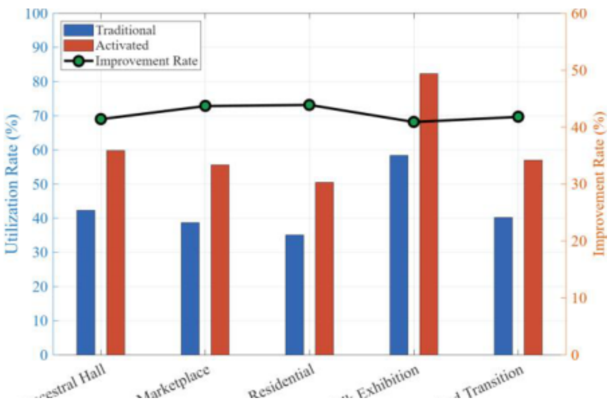

FIGURE 4. Efficiency of Utilizing Intangible Cultural Heritage Space Display

The utilization rates of the five types of activated spaces significantly exceeded the traditional mode, with an average improvement rate of 42.34%, indicating that the improvement of fusion degree has a leverage amplification effect on utilization efficiency. The traditional utilization rate of folk exhibition spaces has the highest base (58.4%), reaching 82.3% after activation, but its improvement rate (40.9%) is slightly lower than the mean, indicating that high base spaces have a marginal decreasing feature of efficiency gains; On the contrary, the traditional utilization rate of residential living space is the lowest (35.1%), but the improvement rate reaches 43.9%, reflecting that daily living space has greater potential for elastic release after cultural gene implantation.

The deep integration of material and non-material cultures is not a simple superposition effect, but presents a three-level catalytic mechanism of “gene anchoring behavior induction efficacy amplification”. The digital cultural genes (pavement patterns, sparrow replacements, column foundations, etc.) are encoded into reusable spatial grammar units through skeleton extraction and shape context clustering. Their precise implantation at core nodes (such as replicating the shape of Ming Dynasty column foundations at ancestral halls and embedding traditional pavement modules in folk exhibition areas) forms a visual and perceptual “cultural anchor”, enhancing the readability and sense of place of the space; This anchoring effect at the material level directly reduces the spatial cognitive threshold of intangible cultural heritage display - users are more likely to identify and stay in areas with high-density gene identification, manifested as a synchronous increase in the duration of stay and interaction frequency in behavioral annotation data.

V. CONCLUSION

This study constructs an activation model for ancient village environmental design based on cultural landscape regeneration, promoting the transformation of ancient village environmental design from empirical intervention to data-driven and dynamically adaptive scientific decision-making paradigm. However, there are still certain limitations to the research: the empirical object is limited to a single regional type, and the transferability of its conclusions in cross-cultural regions needs to be tested through multiple case studies; The dynamic vitality of intangible cultural heritage has not been fully characterized in the quantitative indicator system. In the future, comparative research on multiple types of ancient villages can be expanded, introducing participatory perception data and reinforcement learning frameworks to enable the activation mode to have real-time feedback and adaptive adjustment capabilities, thereby more effectively responding to the continuous changes of complex rural social ecosystems.

REFERENCES

[1] A. Mohajer Milani and H. Assarzadeh, “Assessing the quality of urban environment and landscape of Tajrish Square through Responsive Envi-

ronmental Design," Journal of Sustainable Architecture and Urban Design, vol. 13, no. 1, pp. 27–48, 2025, doi: https://doi.org/10.22061/jsaud.2025.11383.2269.

[2] W. Y. W. Ibrahim, M. S. F. Rosley, and M. A. Abas, "Integrating Spatial Modelling and Interpolation of Environmental Factors in Landscape Design Analysis," International Journal of Advanced Research in Technology and Innovation, vol. 4, no. 2, pp. 18–29, 2022, doi: https://doi.org/10.55057/ijarti.2022.4.2.3.

[3] L. Liu and J. Zhang, "Innovation of Regional Environmental Design Methods under the Background of Rural Revitalization–Taking Ancient Villages in Zhejiang as an Example," Hunan Packaging, vol. 41, no. 2, pp. 89–93, 126, 2026, doi: https://doi.org/10.19686/j.cnki.issn1671-4997.2026.02.021.

[4] L. Chen, "A Study on the Inheritance and Promotion of Planning and Design of Ancient Villages in Huizhou from the Perspective of Rural Revitalization," Journal of Xingtai University, vol. 39, no. 3, pp. 8–13, 2024, doi: https://doi.org/10.3969/j.issn.1672-4658.2024.03.002.

[5] C. Yang and C. Dong, "Analysis of Landscape Renovation Design of Ancient Villages in Huizhou under the Background of Rural Revitalization–Taking Lijia Village in Xihu, Nanchang City as an Example," Anhui Architecture, vol. 30, no. 5, pp. 9, 31, 2023, doi: https://doi.org/10.16330/j.cnki.1007-7359.2023.5.002.

[6] D. Brown and J. Gabrys, "Community-led landscape regeneration: A review of and framework for engagement in restoration initiatives," Ambio, vol. 55, no. 2, pp. 227–244, 2026, doi: https://doi.org/10.1007/s13280-025-02236-3.

[7] A. Barbanente and L. Grassini, "Landscape regeneration and place-based development in marginal areas: learning from an Integrated Project in Southern Salento," City, Territory and Architecture, vol. 11, no. 1, Art. no. 26, 2024, doi: https://doi.org/10.1186/s40410-024-00247-3.

[8] J. N. Tzortzi, L. Guaita, and A. Kouzoupi, "Sustainable strategies for urban and landscape regeneration related to Agri-cultural heritage in the urban-periphery of South Milan," Sustainability, vol. 14, no. 11, Art. no. 6581, 2022, doi: https://doi.org/10.3390/su14116581.

[9] P. Cobeñas, D. Esenarro, J. Vilchez Cairo, et al., "Strategies for the Revalorization of the Natural Environment and Landscape Regeneration at La Herradura Beach, Chorrillos, Peru 2024," Urban Science, vol. 10, no. 1, Art. no. 2, 2025, doi: https://doi.org/10.3390/urbansci10010002.

[10] N. Septian, "Cultural Microcosm in Focus: Landscape and Identity in Small Village Explored Through Design and Environment-Behavior Theories," Environment-Behaviour Proceedings Journal, vol. 9, no. SI23, pp. 259–265, 2024, doi: https://doi.org/10.21834/e-bpj.v9iSI23.6172.

[11] J. Ma and S. A. B. Zakaria, "Incorporating Environmental Sustainability and Supply Chain Management in Contemporary Interior Design: A Study on Chinese Landscape Paintings," Buildings, vol. 14, no. 12, Art. no. 4071, 2024, doi: https://doi.org/10.3390/buildings14124071.

[12] Z. Sadrazamnouri, J. Nouri, F. Habib, et al., "Landscape Planning and Design of Urban Rivers with Environmental Approach (Case Study: Farahzad River Valley in Tehran)," Advanced Environmental Sciences, vol. 20, no. 4, pp. 143–162, 2022, doi: https://doi.org/10.48308/envs.2022.1175.

[13] W. U. You and Z. Ming, "Expansion of Landscape Architecture Body of Knowledge Based on the Regeneration of Urban Built Environment," Landscape Architecture, vol. 31, no. 3, pp. 51–59, 2024, doi: https://doi.org/10.3724/j.fjyl.202310260483.

[14] A. M. Khorasgani and M. Haghighatbin, "Regeneration of historic cities: Reflections of its evolution towards a landscape approach," Journal of the International Society for the Study of Vernacular Settlements, vol. 10, no. 5, pp. 60–78, 2023.